Photochemically Induced Isomerisation of Ruthenium Polypyridyl Complexes

Stefano Fanni,[a] Frances M. Weldon,[a] Leif Hammarström,[b] Emad Mukhtar,[b] Wesley R. Browne,[a] Tia E. Keyes,[c] and Johannes G. Vos*[a]

The synthesis and characterisation of a series of ruthenium polypyridyl complexes containing pyridyltriazole ligands in different coordination modes are described. The electrochemical and electronic properties of the compounds with respect to the coordination mode of the pyridyltriazole ligand are reported. Upon photolysis of the complex containing the 1-methyl-3-(pyridin-2-yl)-1,2,4-triazole ligand, irreversible ligand isomerisation is observed.

Introduction

During the last number of years we have been actively involved in the study of ruthenium and osmium polypyridyl complexes containing ligands with 1,2,4-triazole moieties such as pyridyl-[1] and pyrazyltriazoles.[2] These studies have shown that for dinuclear compounds containing anionic triazolate bridges, strong intercomponent interactions are observed.[3] In addition, mononuclear complexes containing negatively charged triazole rings were found to be photostable.[4] Of further interest in these studies is the inherent asymmetry of the ligands. The nitrogen atoms of the pyridine or pyrazine rings have significantly different electronic properties to the triazole-based nitrogen atoms. In addition the N1 (or N2) and N4 atoms of the triazole ring are non-equivalent, as shown by differences between the acid−base properties of complexes containing N2- and N4-bonded ligands.[1,2] With N-substituted triazole ligands, either N2- or N4-coordination of the ligands is observed, depending on the position of the substituent.[5] Furthermore, it has been shown that for complexes containing neutral pyridyltriazole ligands, photochemically induced isomerisation of the pyridyltriazole ligand can occur.[4,6]

Recently we developed a new synthetic route towards complexes containing N-substituted triazole ligands as shown in Scheme 1.[7]
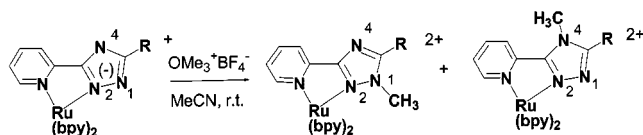
Scheme 1

[a] National Centre for Sensor Research, School of Chemical Sciences, Dublin City University
Dublin 9, Ireland
E-mail: han.vos@dcu.ie
[b] Department of Physical Chemistry, University of Uppsala, Box 532, 75121, Uppsala, Sweden
E-mail: leif.hammarstrom@fki.uu.se
[c] School of Chemistry, Dublin Institute of Technology, Dublin 8, Ireland
E-mail: tia.keyes@dit.ie

In this method, the N2 isomer of a 3-(pyridin-2-yl)-1,2,4-triazole (L1) ruthenium polypyridyl precursor complex (**RuL1N2**) was directly methylated yielding complexes which then contain the ligands 1-methyl-3-(pyridin-2-yl)-1,2,4-triazole (L2) and 4-methyl-3-(pyridin-2-yl)-1,2,4-triazole (L3). Surprisingly, the sterically least favoured complex, **RuL2N2**, methylated at the N2 position; was obtained as the main product, with a yield of about 90%, whereas in the reaction between L2 and [Ru(bpy)$_2$Cl$_2$]·2H$_2$O only the N4 isomer of the complex, **RuL2N4**, could be obtained in appreciable amounts. This new synthetic strategy provided us with the first opportunity to compare their photophysical and photochemical properties and to investigate the role played by steric hindrance. In this paper we report the photochemical and photophysical properties of ruthenium bis(bipyridyl) complexes with the N-substituted triazole ligands L2, L3 and 1,4-bis[1-methyl-3-(pyridin-2-yl)-1,2,4-tri-
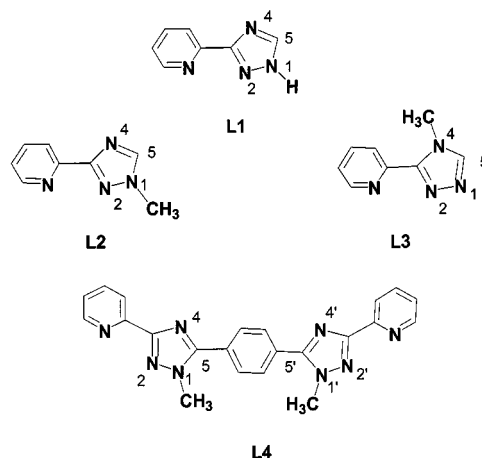

Figure 1. Ligand structures

azol-5-yl]benzene (L4) (see Figure 1). In the latter ligand, both the N2 and N4 sites are sterically hindered. The effect of the benzene and the methyl groups on the composition of the compounds and on their photophysical and photochemical properties were investigated. Emission lifetime, UV/Vis and NMR studies indicate that an irreversible

photoisomerisation takes place, in which the sterically hindered N2-bonded L2 complex is transformed into the N4 species. For the mono- and dinuclear L4 complexes, a less clear picture was obtained, but photoinduced reactions were also observed. The results obtained are discussed with respect to the electronic properties of the compounds.

Results and Discussion

General

An important issue to be addressed first is the coordination mode of the triazole rings in the obtained products, in particular in the L4 complexes. For L2 and L3, the coordination of the triazole ring is known from earlier studies.[1,7] From the reaction mixture of the mononuclear L4 complex, two isomers were isolated by semi-preparative HPLC. In the dinuclear complex, coordination of the two metal units may occur to N2/N2′, N4/N4′ or N2/N4′ of the triazole ring. HPLC analysis of the reaction mixture showed the presence of different isomers. One main isomer was isolated in a pure form by recrystallisation.

¹H NMR Spectroscopy

The position of the methyl signals in the ¹H NMR spectra is diagnostic for the type of isomer obtained (see Table 1). For L2 and L4, the methyl substituent is expected to resonate significantly further upfield than in the free ligand when the ligand is bonded through the N2 atom. This is a consequence of the steric interaction between the methyl group and a neighbouring bpy ligand. For the N4 isomer a smaller shift is expected since no interaction between the methyl group and the bpy ligands is possible.[1,5,8] The methyl resonances recorded for the complexes fall clearly into two groups. The first set of signals at δ ≈ 3.2 is indicative of the presence of steric hindrance, since the values are shifted upfield by about 0.7 ppm, with respect to the free ligand. Such a shift indicates N2 coordination for L2 and L4 complexes. The resonances found at δ ≈ 4 point to coordination modes where the methyl group does not interact with the neighbouring bpy ligands and are indicative of N4 coordination in the L2 and L4 ligands and of N2 coordination in the L3 complex. For the dinuclear L4 complex, only one methyl signal was obtained at δ = 3.23,

Table 1. Chemical shifts (ppm) for methyl groups; measurements were carried out in DMSO unless otherwise stated

Compound	CH₃
RuL2*N2*	3.15 (3.54[a])
RuL2*N4*	3.97 (4.17[a])
RuL3*N4*	4.21
RuL4*N4* (f)	4.07
(b)	3.82
RuL4*N2* (f)	4.10
(b)	3.27
RuRuL4*N2N2*	3.23
(in CD₃CN)	3.17

[a] Measured in acetone; (f) and (b) refer to the free and bound pyridyltriazole ring, respectively.

clearly indicating that both centres are bonded in the same manner, namely through N2.

Redox Properties

All complexes show well-behaved electrochemistry (see Table 2). The redox processes are reversible, with peak-to-peak separations of 60−100 mV. **RuRuL4***N2N2′* exhibits a single, two-electron, metal-based oxidation, without any sign of splitting, indicating that the interaction between the metal centres is at best very weak. The N4-coordinated complexes exhibit somewhat lower Ru$^{II/III}$ potentials than the N2 compounds possibly indicating improved π-acceptor properties of ligands coordinated in the N2 mode. The similarity of the reduction potentials of the compounds reported in this work and those observed for [Ru(bpy)₃]²⁺ suggests that the first reduction process is bpy based. This is further confirmed by the first reduction potential observed for **[Ru(L2***N4*)₃]²⁺ (L2 coordinated through N4) of −1.75 V vs. SCE,[9] approximately 400 mV more negative than that observed for [Ru(bpy)₃]²⁺. This value suggests that the lowest unoccupied molecular orbital (LUMO) in the L2 complex is about 3300 cm⁻¹ higher than in the homoleptic bpy complex.

Table 2. Electrochemical data for the triazole complexes; all measurements were carried out in acetonitrile with 0.1 M TEAP; all redox potentials measurements were performed using ferrocene as an internal reference

Complex	Oxidation potential [V vs. SCE]	Reduction potential [V vs. SCE]
RuL2*N2*	1.30	−1.36, −1.57
RuL2*N4*	1.20	−1.39, −1.61
RuL3*N2*	1.19	−1.39, −1.61
RuL4*N2*	1.31	−1.35, −1.56
RuL4*N4*	1.20	−1.35, −1.58
RuRuL4*N2N2′*	1.29	−1.38, −1.59
[Ru(bpy)₃]²⁺	1.26	−1.35, −1.55, −1.80

Electronic Properties

The absorption spectra bands observed in the 400−460 nm region are associated with dπ−π* MLCT bands. The MLCT bands for complexes containing a *N*4-coordinated triazole ring are found at about the same energy as that of [Ru(bpy)₃]²⁺. In agreement with the electrochemical data, the N2-bonded isomers have an MLCT band at higher energy suggesting that in this coordination mode the σ-donor properties of the L2 and L4 ligands are reduced.

All the compounds show emission at room temperature and at 77 K. The emission lifetimes of the complexes in acetonitrile, measured by time-correlated single-photon counting, are given in Table 3. For **RuL2***N4* and **RuL4***N4*, the major decay component shows a lifetime of 9.0 ns and 35 ns, respectively. A minor (< 5%), faster component has a lifetime of approximately 1 ns. In contrast, for **RuL2***N2* and **RuL4***N2* the 1 ns component was dominant. In these samples, a second slower component was present, and its magnitude varied between 15% and 50% for different meas-

Table 3. UV/Vis absorption and emission data for the complexes; all measurements were carried out in acetonitrile unless otherwise stated

Complex	Absorption λ_{max} [nm] (ε [10^4 M^{-1}cm^{-1}])	Emission λ_{max} [nm] 300 K	77 K[a]	$\tau_{300 K}$ [ns]
RuL2N2	435 (1.15)	615	566	1.0
RuL2N4	452 (1.07)[a]	600[a]	585	9.0
RuL3N2	440 (1.44)[a]	600[a]	584	14.0
RuL4N2	415 (1.33)	611	570	1
RuL4N4	453 (0.90)	614	584	35
RuRuL4N2N2′	414 (2.60)	603	573	1
[Ru(bpy)₃]²⁺	452 (1.30)	615	582	950[b]

[a] Measured in ethanol/methanol (4:1, v/v). − [b] Deaerated solution.

urements. The lifetime of this component matched that of the corresponding N4 isomer. The dimeric **RuRuL4N2N2′** also has a dominant 1 ns component, with a minor slower (32 ns) component that matches the lifetime of **RuL4N4**.

The results obtained from the lifetime measurements for the N2 isomers of L2 and L4 were at first hard to explain, since an impurity level as high as 50% would certainly have been detected by the other characterisation techniques. The formation of a photoproduct seems a more likely explanation for the behaviour observed. For the compounds under investigation, the occurrence of photoinduced ligand processes is not unexpected. It is generally assumed that upon excitation of ruthenium polypyridyl complexes, an electron is transferred from the metal-based ground state to a singlet metal-to-ligand charge-transfer (¹MLCT) state. From this singlet state, the emitting ³MLCT state is populated efficiently by intersystem crossing. Population of the nearby antibonding triplet metal-centred state (³MC) then explains the photoinduced reactivity of the compounds, and in the literature both ligand exchange and rearrangements have been reported.[4,10,11]

To investigate this hypothesis further, a photolysis was carried out in which ¹H NMR spectra were taken after various irradiation times. After irradiating for 6 h in acetonitrile, analysis of the CH₃ resonance suggested that up to 70% of the complex underwent photoinduced isomerisation to the corresponding **RuL2N4** complex. Further irradiation (up to 12 h) resulted mainly in decomposition of the complex **RuL2N2**. This decomposition probably occurs by the formation of a photoinduced intermediate where the pyridyltriazole ligand is coordinated in a monodentate fashion. Such behaviour in strongly coordinating solvents has been reported before for other complexes containing neutral pyridyltriazole ligands.[6b] Under the same conditions, **RuL2N4** shows a remarkable photostability and decomposition becomes noticeable only after 24 h of irradiation. The same experiment was carried out in a weakly coordinating solvent, namely acetone, in an effort to reduce the formation of secondary photoproducts (see Figure 2). Analysis of the methyl region of the spectra shows that the resonance originally obtained for the N2 isomer at δ = 3.54 is replaced by a signal at δ = 4.17 after photolysis. This is indicative of the formation of the N4 isomer, and in acetone typically a 100% photoisomerisation of **RuL2N2** to **RuL2N4** was obtained after irradiation for 30 h. No evidence for the formation of a solvated metal complex was observed. No changes

were observed in the ¹H NMR spectra of **RuL2N4** after irradiating for 24 h. These results suggest that irreversible photoinduced isomerisation of **RuL2N2** to **RuL2N4** is taking place as shown in Scheme 2.
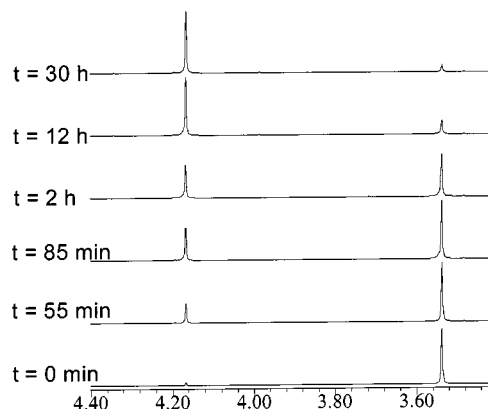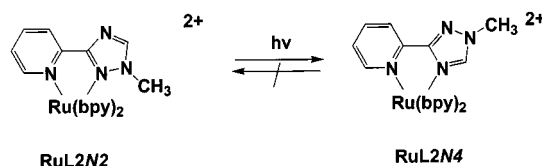

Figure 2. ¹H NMR spectra of the methyl region taken during photolysis of **RuL2N2** in [D₆]acetone

Scheme 2

This photoisomerisation process can also be observed using UV/Vis absorption spectroscopy. As can be seen in Figure 3, irradiation of **RuL2N2** in acetone causes a gradual decrease in intensity of the band at 415 nm and a concomitant growth of bands at 355 nm and 455 nm, which are associated with the **RuL2N4** complex (Table 3). The UV/Vis spectra show isosbestic points at 448 nm and 372 nm, indicating that photoproducts are formed directly without the production of long-lived intermediates. Upon complete photolysis, no further changes in the absorption spectrum occur, which further indicates the photostability of **RuL2N4**.
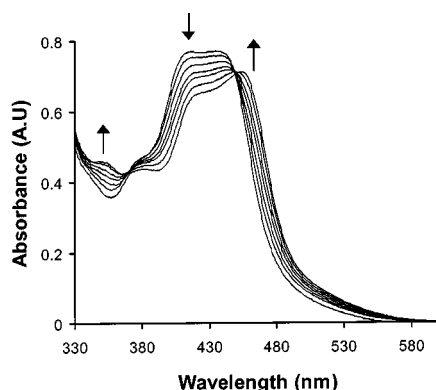
Figure 3. UV/Vis absorption spectra of **RuL2*N2*** in acetone upon irradiation for (a) 0 min, (b) 2.5 min, (c) 5 min, (d) 10 min, (e) 17.5 min, (f) 27.5 min, (g) 120 min

The conclusions drawn from the NMR and UV/Vis studies were further corroborated by emission lifetime measurements on **RuL2*N2*** in acetonitrile exposed to varying amounts of light. The results are shown in Figure 4. To minimise exposure of the sample to light during the lifetime measurements, these were continued for only 2−3 min (giving 1000 counts in the peak channel). In the first measurement, the contribution from the longer lived N4 isomer emission was only 15%. However, after only a few minutes of subsequent irradiation with a 450-W Xe lamp (using a water heat filter and a $\lambda > 385$ nm cut-off), this contribution had increased to 80%, indicating an almost complete conversion into the N4 isomer. When irradiation was continued, an instrument-response limited component ($\tau < 150$ ps) started to appear (not shown), and after 100 min of irradiation very little of the N4 isomer remained. We attribute the very short-lived component to the photolysed complex in which the L2 ligand had presumably been replaced by acetonitrile.
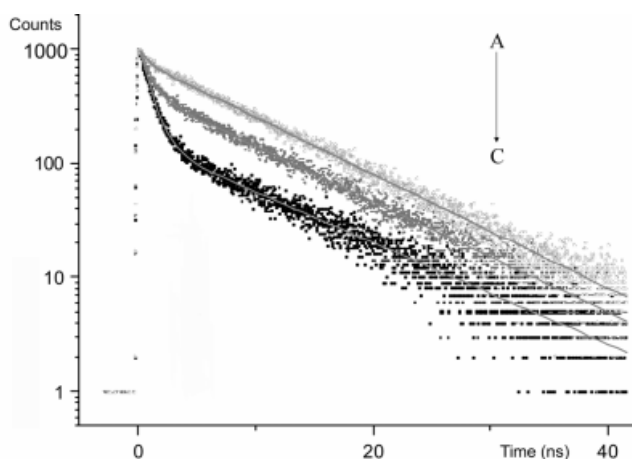
Since **RuL4*N2* and RuRuL4*N2N2*′** also showed a double-exponential emission decay, NMR experiments were also carried out for the L4 compounds. For all three complexes, irradiation in acetone resulted in a complex mixture of products, which could be attributable to partial isomerisation and decomposition of the starting material and products. The results obtained from these experiments were not further analysed.

Concluding Remarks

The results obtained in this investigation demonstrate the importance of steric factors in the photochemical properties of ruthenium polypyridyl compounds. Earlier studies[4] have shown that for the protonated L1 complexes, a *reversible* N2/N4 photoinduced isomerisation is taking place. The results obtained for the L2 complex indicate that sterically hindered complexes (i.e. **RuL2*N2***), have the tendency to release the steric congestion upon photolysis by converting into the corresponding unhindered isomer (i.e. **RuL2*N4***). The presence of a steric constraint in the compound therefore leads to an *irreversible* photoisomerisation.

Pyridyltriazoles are mainly σ-donor ligands and have only limited π-acceptor properties. Therefore it seems likely that the small differences observed in the electronic spectra and in the Ru$^{II/III}$ redox potentials of the different isomers can be explained by a reduced σ-donor capability of the N2 isomer owing to steric hindrance. This leads to a lower excited-state ^{3}MC level in the N2 isomer than in the N4 isomer and facilitates the photochemically induced isomerisation of the N2 isomer by a photochemically driven process.

When substituents are present at both the N1 and C5 positions (as in the three L4 complexes), neither of the possible isomers is sterically unhindered. Hence, irradiation of these complexes results in a mixture of different isomers of similar stability (or, in other words, "photochemical instability").

Experimental Section

Materials: All synthetic reagents were of commercial grade and no further purification was employed, unless otherwise stated. All solvents employed in spectroscopic and electrochemical measurements were of HPLC or spectroscopic grade.

Experimental Methods: ^{1}H NMR spectra were recorded with a Bruker AC400 (400 MHz) instrument. For NMR-scale photochemical experiments, 5−10 mg of a given complex was dissolved in [D$_3$]acetonitrile or [D$_6$]acetone (0.5 mL), placed in a borosilicate NMR tube and irradiated using a 150-W halogen lamp. NMR spectra were taken at regular intervals and the degree of isomerisation checked by integration of the CH$_3$ resonance signals. − UV/Vis spectra (accuracy ± 2 nm) were obtained using a Shimadzu UV3100 UV/Vis−NIR spectrophotometer interfaced to an Elonex PC433 personal computer. The estimated error of the extinction coefficients is 5%. − Emission spectra (accuracy ± 5 nm) were obtained with a Perkin−Elmer LS50B luminescence spectrometer

Figure 4. Emission decays for the same sample of **RuL2*N2*** in acetonitrile; curve A: sample prepared in the dark; curve B: after 1.5 min of irradiation with an Xe lamp; curve C: after 6.5 min of irradiation; the lines are double-exponential fits to the data, with lifetimes of 1.0 ns and 9.0 ns; the contribution from the slower component increased from 15% in A to 40% in B and 80% in C

equipped with a red-sensitive Hamamatsu R928 detector, interfaced with an Elonex PC466 personal computer employing Perkin−Elmer FL WinLab custom-built software. At room temperature, unless otherwise indicated, acetonitrile was the solvent used, and excitation and emission slit widths of 10 nm, were employed. At 77 K measurements were carried out in ethanol/methanol (4:1, v/v) using excitation and emission slit widths of 5 nm. The spectra were not corrected for the photomultiplier response. − For electrochemical measurements, HPLC grade acetonitrile dried with molecular sieves was employed. Potentials are ± 50 mV. The electrolyte used was 0.1 M tetraethylammonium perchlorate (TEAP). The electrochemical cell used was a conventional three-compartment cell with glass frits. The reference electrode used was a saturated calomel electrode. The working electrode was a 3-mm diameter teflon shrouded glassy carbon electrode and a platinum gauze was employed as the counter electrode. Prior to reduction measurements, the solutions were degassed for 15 min with nitrogen. Cyclic voltammetry (100 mVs^{-1}) was carried out using a CH instruments Model 660 electrochemical workstation interfaced to an Elonex 486 PC. Analytical HPLC experiments were carried out using a Waters HPLC system, consisting of a model 501 pump, a 20-µL injector loop, a Partisil SCX radial PAK cartridge mounted in a radial compression Z module and a Waters 990 photodiode array detector. An NEC APCIII computer controlled the system. The detection wavelength used was 280 nm and the flow rate was 2.0 mL/min. The mobile phase was CH_3CN/H_2O (80:20) containing 0.1 M $LiClO_4$. Semipreparative HPLC was carried out using an ACS pump, a 1-mL injection loop and a Waters Partisil SCX 10 µm cation exchange column (25 × 100 mm). The mobile phase used was $CH_3CN:H_2O$ (80:20) containing KNO_3 (0.12−0.20 M). The flow rate used varied between 1.50 and 2.0 mL/min.

Single-Photon Counting: Fluorescence lifetimes were determined using time-correlated single-photon counting. The excitation source had a tuneable output of a 200 kHz and a 120 femtosecond optical parametric amplifier (OPA, Coherent Radiation Inc). This device was pumped by a regenerative amplifier (700 µJ, 150 fs, 200 kHz) seeded by the 80 fs output of a Ti:Sapphire oscillator. The frequency-doubled fundamental generated in the OPA was used to excite the samples at 400 nm. A polariser was located before the sample to define the vertical polarisation of the excitation light and all fluorescence measurements were carried out with an analysing polariser before the detector was oriented at the magic angle (54.7°), relative to the excitation polarisation, to remove anisotropy effects. Fluorescence was observed through an interference filter centred at 600 nm (Oriel, USA) with a full-width at half-maximum of 10 nm. A microchannel plate multiplier (Hamamatsu) was used for the detection. Instrumental response curves were measured by exchanging the 600 nm interference filter after the sample with a 400 nm filter and recording the scattering from a scatter solution. The instrumental response (FWHM) was ca. 100 ps. The fluorescence decay data were analysed with a nonlinear least-squares program using a modified Levenberg−Marquardt algorithm with iterative reconvolution. The reduced χ^2 and residual plots were used to judge the quality of the fits. The samples for emission lifetime measurements were dissolved in spectroscopic grade acetonitrile (Merck) to an optical density of ca. 0.3 at the excitation wavelength. The solvents were not degassed since quenching by O_2 had negligible effect on the short lifetimes measured. Lifetimes are ± 10%.

Ligand Synthesis

Synthesis of 1,4-Bis[1-methyl-3-(2-pyridyl)-1,2,4-triazol-5-yl]benzene (L4)

Step 1. Synthesis of *N2*-methyl-2-pyridylamidrazone: 2-Cyanopyridine (36 g, 0.35 mol) and excess methylhydrazine (18.43 g, 0.40 mol) were mixed in a minimum amount of ethanol and allowed to stir overnight. The pale yellow crystalline product was filtered, washed with diethyl ether and air dried. Yield 26.7 g (50%). − M.p. 108−110 °C (ref.[12] 109−110 °C). − ^{1}H NMR ($CDCl_3$): δ = 7.24 (1 H, dd, pyridyl H^5), 7.67 (1 H, dd, pyridyl H^4), 8.08 (1 H, d, pyridyl H^3), 8.50 (1 H, d, pyridyl H^6), 5.24 (2 H, br. s, NH), 2.98 (3 H, s, CH_3). − ^{13}C NMR ($CDCl_3$): δ = 38.48, 119.60, 123.32, 136.02, 146.41, 147.77, 150.72.

Step 2. Synthesis of *N,N′*-Terephthaloylbis[(*N2*-methyl-2-pyridyl)hydrazide]: This intermediate was prepared by the dropwise addition of a THF solution (30 cm^3) of terephthaloyl dichloride (5.08 g, 0.025 mol) to a solution of *N2*-methyl-2-pyridylamidrazone (7.50 g, 0.05 mol) and triethylamine (10 cm^3) in THF while maintaining the reaction mixture at 0°C. The reaction mixture was then reduced to approximately 25 mL and an equal volume of water was added. The yellow product was filtered, washed with water, hot methanol and diethyl ether, dried under vacuum and then left in an oven at 60 °C for 24 h. Yield 7.00 g (65%). − M.p. 178−180 °C. − ^{1}H NMR ($CDCl_3$): δ = 8.15 (2 H, s, phenyl), 8.10 (1 H, d, pyridyl H^3), 7.65 (1 H, dd, pyridyl H^4), 7.43 (1 H, dd, pyridyl H^5), 8.60 (1 H, d, pyridyl H^6), 10.30 (1 H, br. s, NH), 4.11 (3 H, s, CH_3). − ^{13}C NMR ($CDCl_3$): δ = 38.50, 120.82, 124.67, 128.85, 129.10, 136.89, 148.24, 150.26, 153.79, 161.2.

Step 3. Cyclization of *N,N′*-Terephthaloylbis[(*N2*-methyl-2-pyridyl)hydrazidine] to Form L3: *N,N′*-Terephthaloylbis[(*N2*-methyl-2-pyridyl)hydrazidine] (7.00 g, 0.017 mol) was suspended in a minimum volume (ca. 30 mL) of ethylene glycol and heated at reflux for 2 h. A white crystalline precipitate was obtained upon cooling of the solution. Further precipitation of the product was induced by the addition of a small amount of water to the mother liquor. The ligand was recrystallised from boiling methanol, filtered and dried under vacuum overnight. Yield 4.20 g (66%). − M.p. 278−280 °C. − ^{1}H NMR ($CDCl_3$): δ = 8.07 (2 H, s, phenyl), 8.10 (1 H, d, pyridyl H^3), 7.92 (1 H, dd, pyridyl H^4), 7.45 (1 H, dd, pyridyl H^5), 8.67 (1 H, d, pyridyl H^6), 4.12 (3 H, s, CH_3). − ^{13}C NMR ($CDCl_3$): δ = 37.65, 121.58, 124.15, 129.00, 129.13, 137.16, 149.45, 149.71, 154.26, 159.88. − MS; *m/z*: 395 [M + 1]$^+$. − $C_{22}H_{18}N_8$: calcd. C 66.98, H 4.60, N 28.41; found C 66.69, H 4.61, N 27.95.

Synthesis of Metal Complexes: *cis*-[Ru(bpy)$_2$Cl$_2$]·2H$_2$O[13] was prepared as reported in the literature. **RuL2*N4*** and **RuL3*N2*** were prepared as reported before.[1] **RuL2*N2*** was prepared by direct methylation[7] of **RuL1*N2*.[1]

Synthesis of [Ru(bpy)$_2$L4](PF$_6$)$_2$: L4 (0.789 g, 2 mmol) was dissolved in hot methanol/water (2:1, v/v). To the solution was added *cis*-[Ru(bpy)$_2$Cl$_2$]·2H$_2$O (0.312 g, 0.6 mmol) and the mixture was heated at reflux for 6 h. Following the removal of most of the solvent by rotary evaporation and the addition of saturated aqueous NH$_4$PF$_6$ solution, the resulting precipitate was filtered and dried. HPLC analysis revealed the presence of two isomers in a 30:70 ratio (isomer 1/isomer 2). These were obtained in a pure form by semipreparative HPLC using acetonitrile/water (80:20) containing 0.11 M KNO$_3$ as the mobile phase and a flow rate of 1.7 mL/min. Total yield after purification (isomer 1 + isomer 2): 0.20 g (30%).

Isomer 1 (RuL4*N4*): $C_{42}H_{34}F_{12}N_{12}P_2Ru·3H_2O$: calcd. C 45.78, H 3.50, N 14.58; found C 45.24, H 3.12, N 14.14.

Isomer 2 (RuL4*N2*): $C_{42}H_{34}F_{12}N_{12}P_2Ru·H_2O$: calcd. C 45.19, H 3.23, N 15.06; found C 45.41, H 3.15, N 14.93.

Synthesis of [(Ru(bpy)₂)₂L4](PF₆)₄·3H₂O (RuRuL4*N2N2′***):** *cis*-[Ru(bpy)₂Cl₂]·2H₂O (0.624 g, 1.2 mmol) and L4 (0.197 g, 0.5 mmol) were heated at reflux in ethanol/water (2:1, v/v) for 6 h. Upon cooling of the reaction mixture, a few drops of a saturated aqueous solution of ammonium hexafluorophosphate were added, whereupon a bright orange precipitate was obtained. This was filtered and recrystallised from acetone/water (2:1, v/v). HPLC analysis of the product showed the presence of only one isomer. Yield 0.30 g (33%). − $C_{62}H_{50}F_{24}N_{16}P_4Ru_2$·3H₂O: calcd. C 40.11, H 3.04, N 12.07; found C 40.27, H 3.08, N 12.02.

[1] [1a] R. Hage, R. Prins, J. G. Haasnoot, J. Reedijk, J. G. Vos, *J. Chem. Soc., Dalton Trans.* **1987**, 1381. [1b] B. E. Buchanan, J. G. Vos, M. Kaneko, W. J. M. van der Putten, J. M. Kelly, R. Hage, R. A. G. de Graaff, R. Prins, J. G. Haasnoot, J. Reedijk, *J. Chem. Soc., Dalton Trans.* **1990**, 2425.

[2] [2a] R. Hage, J. G. Haasnoot, H. A. Nieuwenhuis, J. Reedijk, R. Wang, J. G. Vos, *J. Chem. Soc. Dalton Trans.* **1991**, 3271. − [2b] H. A. Nieuwenhuis, J. G. Haasnoot, R. Hage, J. Reedijk, T. L. Snoeck, D. J. Stufkens, J. G. Vos, *Inorg. Chem.* **1991**, *30*, 48. − [2c] T. E. Keyes, C. M. O'Connor, U. O'Dwyer, C. G. Coates, P. Callaghan, J. J. McGarvey, J. G. Vos, *J. Phys. Chem. A* **1999**, *103*, 8915.

[3] R. Hage, J. G. Haasnoot, H. A. Nieuwenhuis, J. Reedijk, D. J. A. De Ridder, J. G. Vos, *J. Am. Chem. Soc.* **1990**, *112*, 9245.

[4] R. Wang, J. G.Vos, R. H. Schmehl, R. Hage, *J. Am. Chem. Soc.* **1992**, *114*, 1964.

[5] E. M. Ryan, R. Wang, J. G. Vos, R. Hage, J. G. Haasnoot, *Inorg. Chim. Acta* **1993**, *208*, 49.

[6] [6a] B. E. Buchanan, H. Hughes, J. H. van Diemen, R. Hage, J. G. Haasnoot, J. Reedijk, J. G. Vos, *J. Chem. Soc, Chem Commun.* **1991**, 300. − [6b] B. E. Buchanan, P. Degn, J. M. Pavon Velasco, H. Hughes, B. S. Creaven, C. Long, J. G. Vos, R. A. Howie, R. Hage, J. H. van Diemen, J. G. Haasnoot, J. Reedijk, *J. Chem. Soc., Dalton Trans.* **1992**, 1177.

[7] S. Fanni, S. Murphy, J. S. Killeen, J. G. Vos, *Inorg. Chem.* **2000**, *39*, 1320.

[8] P. J Steel, F. Lahousse, D. Lerner, C. Marzin, *Inorg. Chem.* **1983**, *22*, 1488.

[9] R. Hage, Ph. D Thesis, Leiden University, **1991**.

[10] [10a] S. Tachiyashiki, H. Ikezawa, K. Mizumachi, *Inorg. Chem.* **1994**, *33*, 623. − [10b] R.Arakawa, S. Tachiyaskiki, T. Matsuo, *Anal. Chem.* **1995**, *67*, 4138.

[11] A. Juris, V. Balzani, F. Barigelletti S. Campagna, P. Belser, A. von Zelewsky, *Coord Chem. Rev.* **1988**, *84*, 85.

[12] S. Kubota, M. Uda, T. Nakagawa, *J. Heterocycl. Chem.* **1975**, *12*, 855.

[13] B. P. Sullivan, D. J. Salmon, T. J. Meyer, *Inorg. Chem.* **1978**, *17*, 3334.